58. Complexes of 2,2′,2″-Nitrilotriphenol

Part 1

A Study of Bimolecular Nucleophilic Substitution at the Boron Atom

by **Edgar Müller**[1]) and **Hans-Beat Bürgi**[2])*

Laboratorium für Anorganische Chemie, ETH, CH-8092 Zürich

(6. II. 87)

The tetradentate ligand 2,2′,2″-nitrilotriphenol forms a boron complex **III** with an intramolecular, transannular N→B dative bond of 1.68 Å in a strained tricyclo[3.3.3.0]undecane chelating system. The complex reacts with nitrogen bases L, such as pyridine, quinuclidine and others, to form complexes **III**-L, in which the intramolecular B–N bond is replaced by one between B and the external nucleophile. In solution, this displacement reaction is reversible. It was studied by temperature-dependent NMR spectroscopy. The resulting reaction and activation parameters suggest that the reaction is a bimolecular nucleophilic substitution (S_N2).

Introduction. – Boron(III) complexes with electronegative ligand atoms like N-, O-, or halogen atoms usually show coordination numbers 3 or 4. To our knowledge, coordination number 5 has not been observed in such environments. It seemed of interest to see whether the coordination of B(III) resembles that of the neighbouring C-atom in the same row of the periodic table or that of the Si-atom which is diagonally related to it. The C-atom shows coordination numbers 1 to 4 in stable compounds, coordination number 5 being adopted only in metastable transition states of S_N2 reactions. The Si-atom, on the other hand, forms stable four-, five-, and even six-coordinate compounds with electronegative ligands.

In an attempt to answer this question, we chose to investigate boron complexes with known tetradentate tripod-type ligands and especially their reactivity towards N-nucleophiles:

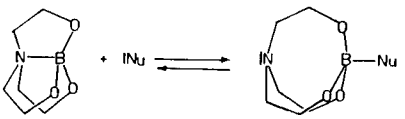

Some complexes with tripod ligands have been described, *e.g.* the boron complexes of nitrilotriethanol (**I**) and nitrilotriacetic acid (**II**). These show transannular B–N bond distances of 1.667 Å [1] and 1.620 Å [2], respectively, which are long compared to the B–N bond distance of 1.57 Å found in cubic boronitride [3]. Enhanced reactivity of these

[1]) Present address: Département de chimie minérale, analytique et appliquée, Université de Genève, 30, quai Ernest Ansermet, CH-1211 Genève 4.

[2]) Present address: Laboratorium für chemische und mineralogische Kristallographie, Universität Bern, Freiestr. 3, CH-3012 Bern.

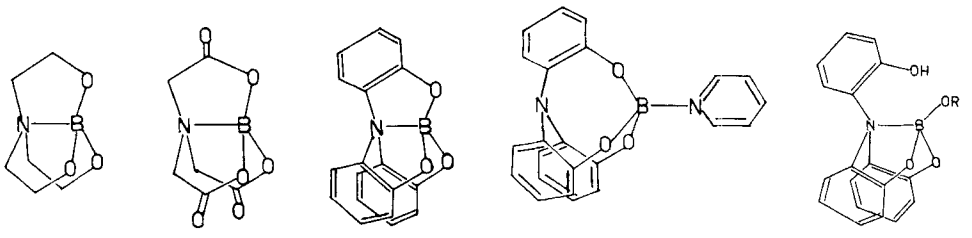

I II III IV V

compounds towards nucleophilic substitution at the B-atom could, therefore, be expected. However, both compounds were unsuitable for corresponding experiments: **II** is insoluble in the common aprotic solvents [2]; **I** is soluble but shows no reactivity towards moderate nucleophiles such as pyridine, diazabicyclooctane, *etc.* However, the boron complex **III** of the known ligand 2,2′,2″-nitrilotriphenol [4] was found to form adducts with N-bases. Compound **III** and its adducts with pyridine (see **IV**) and 1-azabicyclo[2.2.2]octane were studied by X-ray crystallography [5] and the reaction **III** + Py⇄**IV** (Py = pyridine) characterized by NMR spectroscopy.

Synthesis and Reactivity of III. – The ligand 2,2′,2″-nitrilotriphenol is obtained as described by *Frye et al.* [4]. Compound **III** is synthesized by mixing solutions of trimethyl borate and the ligand in a convenient solvent at room temperature. Aprotic solvents like $CHCl_3$, MeCN, or THF are recommended. The formation of **III** was followed by ^{1}H-NMR spectroscopy: After mixing solutions of the ligand and of $(MeO)_3B$ in $CDCl_3$ at room temperature, the spectrum first shows an intermediate product. After some min, formation of **III** begins, and short heating to 60° is sufficient to complete the reaction. Structure **V** is assigned to the intermediate (R = CH_3). Attempts to synthesize or recrystallize **III** in alcohols gave only intermediate **V** (^{1}H-NMR). An analogous intermediate has been observed during synthesis and attempted recrystallization of **II** [2].

Alternatively, **III** may be prepared by heating 2,2′,2″-nitrilotriphenol and $B(OH)_3$. Compound **III** can be sublimed *in vacuo*.

If the synthesis or recrystallization of **III** is carried out in pyridine as a solvent, a 1:1 adduct **IV** with pyridine is isolated. Analogous adducts are obtained with quinuclidine (Quin), diazabicyclooctane (DABCO), and 4-(dimethylamino)pyridine (Me_2NPy) from $CHCl_3$, Me_3CN, or THF solutions. No crystalline adducts could be obtained with 2-methylpyridine, 2,6-dimethylpyridine, quinoline, pyridine-4-carbonitrile, Et_3N, Ph_3N, and azatrypticene (N-donors), *tert*-butyl isocyanide (C-donor), Ph_3P, the 'cage phosphite' 1-phospha-2,6,7-trioxabicyclooctane (P-donors), and Ph_3As (As-donor). Note, however, that 2-methylpyridine or pyridine-4-carbonitrile increase the solubility of **III** in MeCN or THF considerably: the effect is more pronounced in the cold than in the warm. Both observations indicate adduct formation in these solutions (see below).

Upon heating, the crystalline adduct **IV** looses pyridine and turns into crystalline **III**. This solid-state reaction may be followed as a function of temperature with the help of X-ray powder diagrams *(Fig. 1)*. The adduct **IV** expels pyridine at ~ 90°. An intermediate phase appears, which undergoes a second transformation at about 180° *(Fig. 1a)*. The resulting end product is identical with genuine **III**, which shows the same powder pattern in the entire temperature range 90–250° *(Fig. 1b)*. If **IV** is heated to 110° until all pyridine is lost and then cooled to room temperature, the intermediate phase

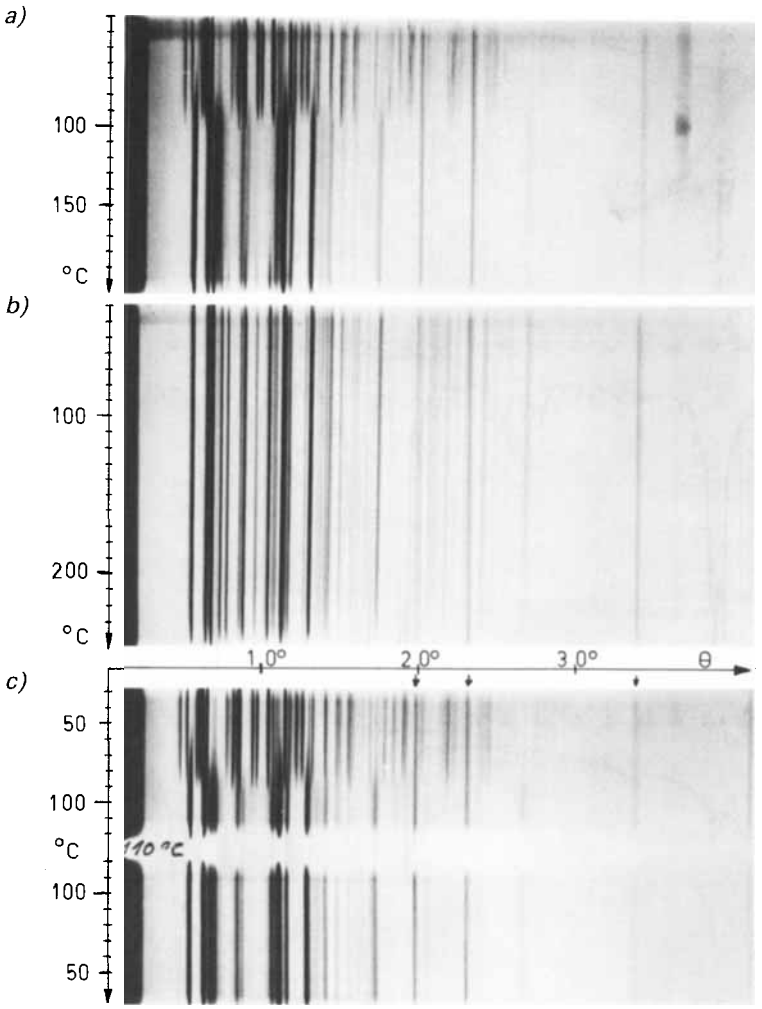

Fig. 1. *Powder diagrams of* **III** *and* **IV** *as a function of temperature* (see text)

persists *(Fig. 1c)*. It is found to be chemically identical to **III** by IR spectroscopy. The second transformation at 180°, thus, seems to be a recrystallization process. A similar behaviour is observed for the adducts of **III** with DABCO and with quinuclidine. In both cases, the bases are expelled at about 180°, the solid product being **III**.

IR Spectra. – The IR spectra of both **III** *(Fig. 2a)* and **IV** *(Fig. 2c)* show weak aromatic C–H stretching modes above 3000 cm^{-1} and a series of intense, sharp absorption bands in the fingerprint region (< 1500 cm^{-1}). The spectrum of **IV** *(Fig. 2c)* is not simply a superposition of the spectra of **III** and of pyridine *(Fig. 2b)*; there is a distinct difference between the spectra of **III** and **IV**, especially in the regions 760–980 cm^{-1} and 1240–1430 cm^{-1}, where pure pyridine does not absorb. As a consequence, the adduct cannot be considered as **III** with a pyridine molecule of crystallization.

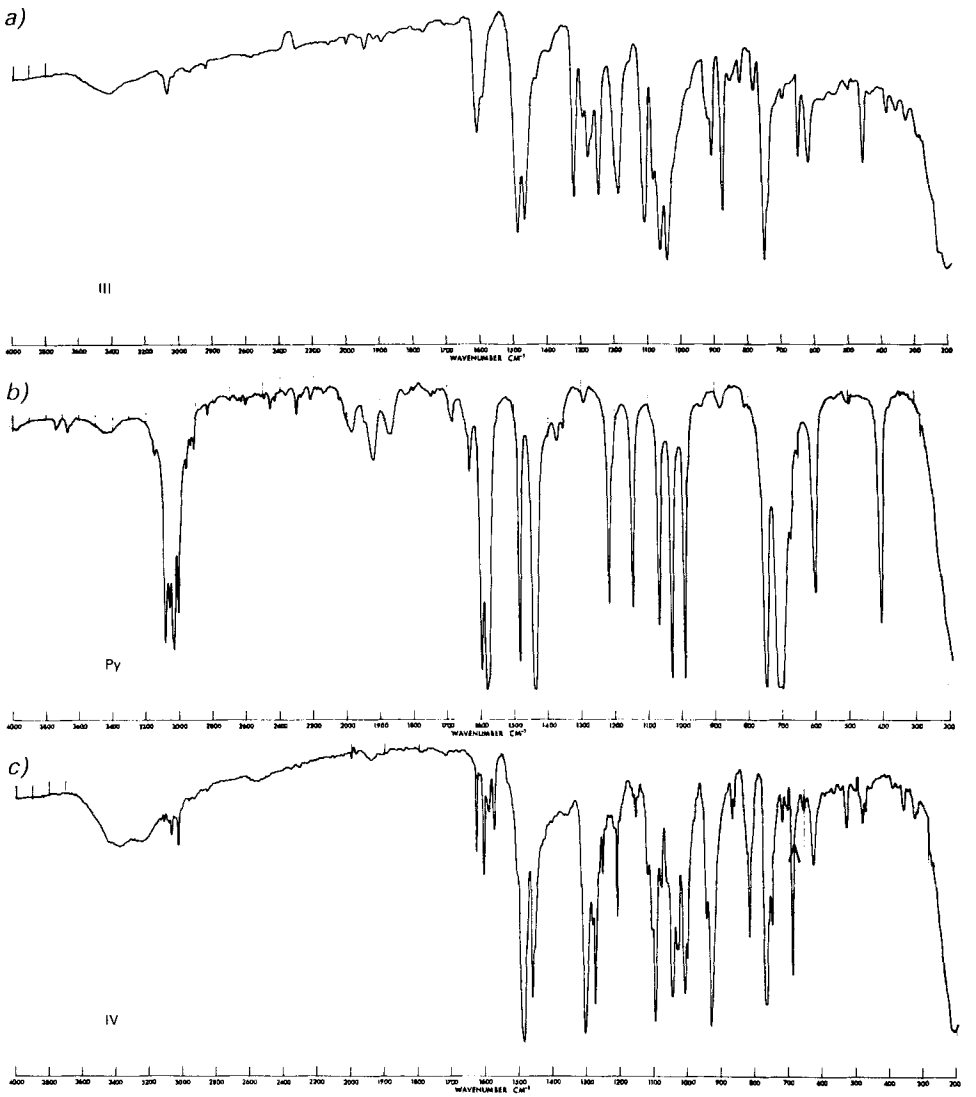

Fig. 2. *IR spectra of* (a) **III**, (b) *Py, and* (c) **IV**

NMR Spectra. – In analogy to the IR spectra, the ^{1}H-NMR spectrum (250 MHz) of **III** in (D_8)THF is distinctly different from the low-temperature ^{1}H-NMR spectrum of **IV** in the same solvent. Again, the low-temperature spectrum of **IV** *(Fig. 3a)* is not a superposition of the spectra of **III** and pyridine, indicating the presence of an adduct as implied in formula **IV**. Upon heating, the various signals of **IV** coalesce in the temperature range 270–320 K *(Fig. 4)*. At temperatures $\geqslant$ 350 K, the spectrum may be understood completely as a superposition of the spectra of **III** and of free pyridine *(Fig. 3b)*. This finding is interpreted in terms of a temperature-dependent equilibrium **III** + Py$\rightleftharpoons$**IV**.

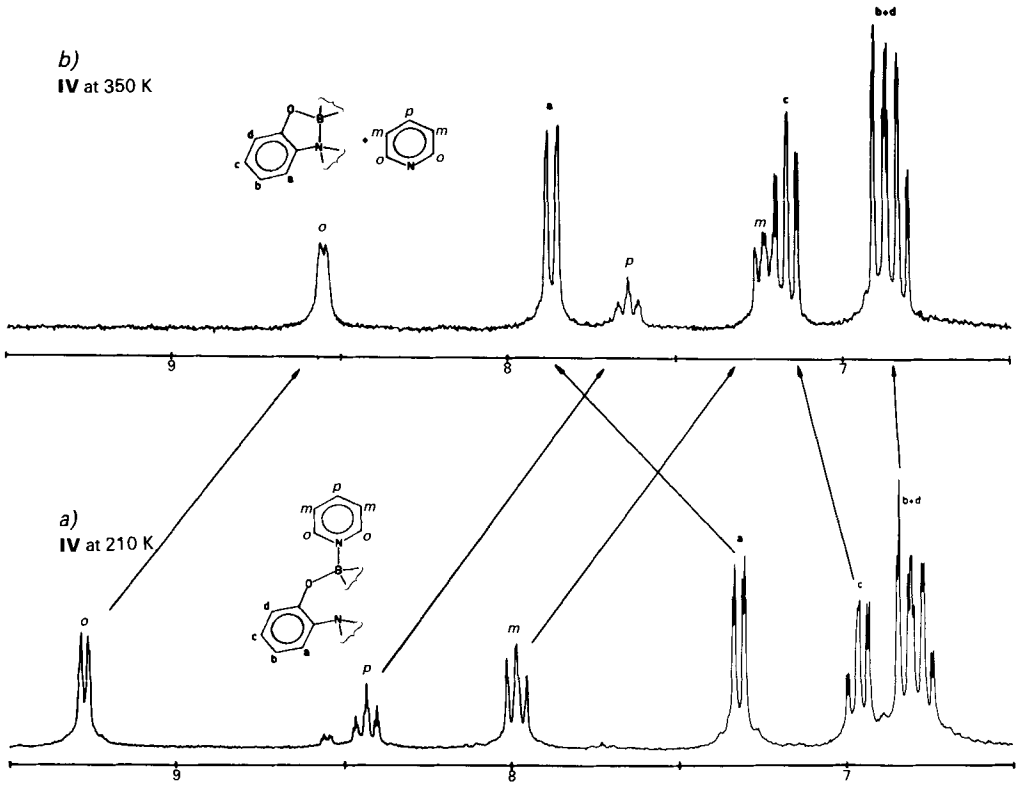

Fig. 3. *250-MHz ^{1}H-NMR spectra of* **IV** *in (D_8)THF at* (a) *210 K and* (b) *350 K* (6.5-to-9.5-ppm region, relative to TMS)

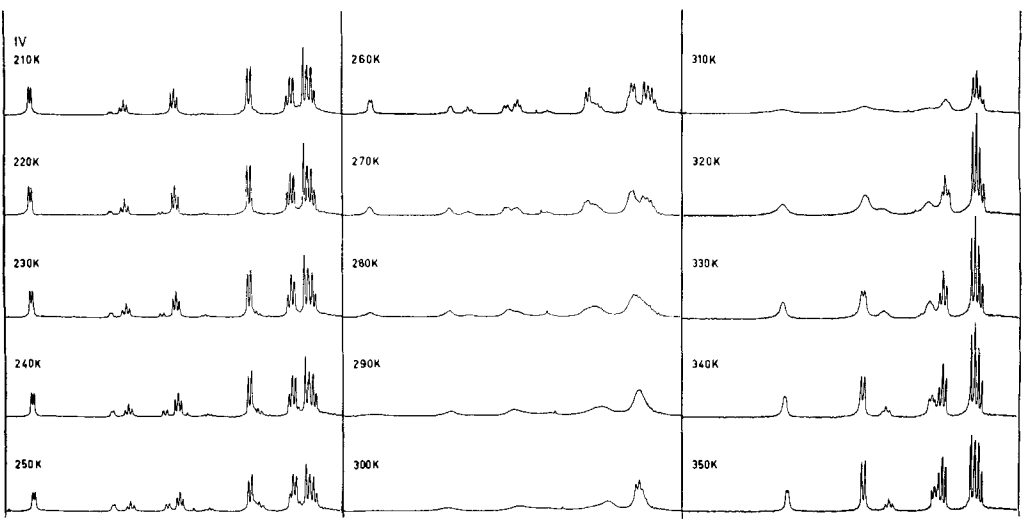

Fig. 4. *250-MHz ^{1}H-NMR spectra of* **IV** *between 6.5 and 9.5 ppm at different temperatures*

This interpretation is confirmed by ^{11}B-NMR spectra (80.25 MHz): below 210 K, a single line at +5.6 ppm (rel. to external $BF_3 \cdot OEt_2$) is observed. When the temperature is raised, the intensity of this signal decreases, and at the same time a second signal appears at +19.4 ppm. Above 350 K, only the latter signal is observed.

X-Ray Structures. – The structures of both **III** and **IV** have been elucidated by single crystal X-ray methods [5]. The complex **III** *(Fig. 5)* is a molecular compound with approximate C_{3v} symmetry; it shows a transannular N→B dative bond of length 1.681(5)

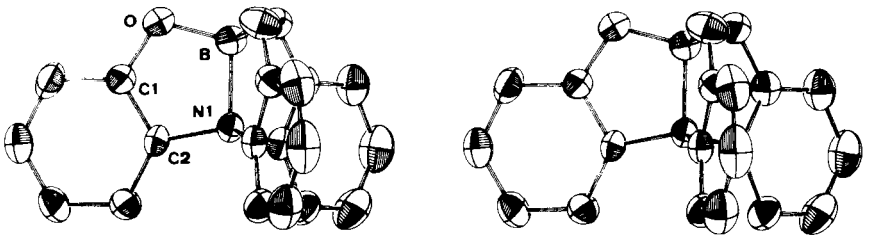

Fig. 5. *Stereoscopic drawing of the* **III** *molecule*

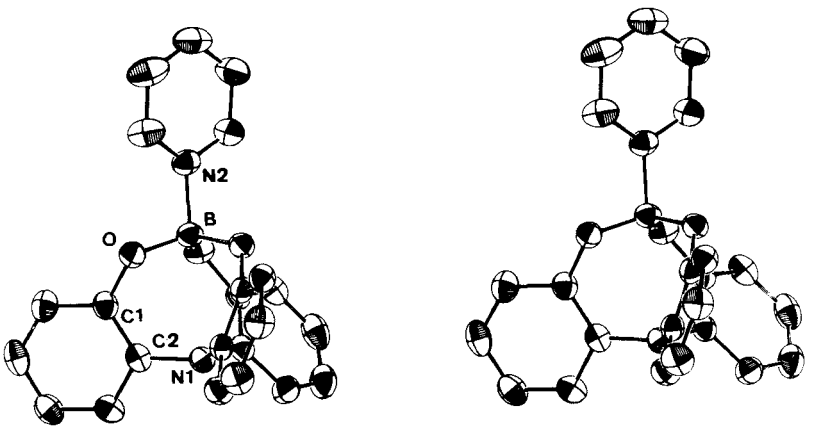

Fig. 6. *Stereoscopic drawing of the* **IV** *molecule*

Table 1. *Geometric Parameters of* **III** *and* **IV** *Averaged with Respect to the Molecular 3-Fold Axis.* E.s.d.'s estimated as $(\sum_3 \sigma_i^2/3)^{1/2}$.

	III	IV		III	IV
B–O	1.443(16) Å	1.451(3) Å	N(1)–B–O	103.9(3)°	–
O–C(1)	1.356(9) Å	1.363(3) Å	N(2)–B–O	–	103.7(2)°
C(1)–C(2)	1.377(6) Å	1.393(4) Å	O–B–O	114.4(3)°	114.5(2)°
C(2)–N(1)	1.470(18) Å	1.434(3) Å	C(2)–N–C(2)	116.4(2)°	118.0(2)°
B(1)–B	1.681(5) Å	2.816(4) Å			
N(2)–B	–	1.631(4) Å	N(1)–B–O–C(1)	–5.3(4)°	–38.5(23)°
			B–O–C(1)–C(2)	3.8(9)°	42.5(39)°
B–O–C(1)	109.4(3)°	120.9(2)°	O–C(1)–C(2)–N(1)	0.0(11)°	2.6(34)°
O–C(1)–C(2)	115.7(3)°	121.5(2)°	C(1)–C(2)–N–B	–3.1(9)°	19.7(22)°
C(1)–C(2)–N(1)	109.6(3)°	121.1(2)°	C(2)–N(2)–B–O	5.0(5)°	32.7(16)°
C(2)–N(1)–B	101.1(2)°	81.8(2)°			

Å. The adduct **IV** *(Fig. 6)* shows a pyridine ligand attached to the B-atom with a B–N distance of 1.631(4) Å. The N-atom of the tripod ligand is detached from the B-atom and is found at a distance of 2.816(4) Å. *Table 1* shows selected geometric parameters of the molecules **III** and **IV**, averaged with respect to the approximate molecular threefold axes.

Equilibrium and Activation Parameters. – The dissociation reaction:

$$\mathbf{IV} \underset{k_2}{\overset{k_1}{\rightleftharpoons}} \mathbf{III} + \mathrm{Py}$$

may be characterized in terms of its equilibrium constant

$$\mathrm{K} = \frac{[\mathbf{III}][\mathrm{Py}]}{[\mathbf{IV}]} = c_0 \frac{x^2}{(1-x)}$$

where c_0 is the known total concentration:

$$c_0 = [\mathbf{IV}] + [\mathrm{Py}] = [\mathbf{IV}] + [\mathbf{III}]$$

and x is the mole fraction, as obtained from the integrated NMR signals of **III**, Py, and **IV**:

$$x = \frac{[\mathbf{III}]}{([\mathbf{III}] + [\mathbf{IV}])} = \frac{[\mathrm{Py}]}{([\mathrm{Py}] + [\mathbf{IV}])}$$

as well as of its rate constants for the forward reaction:

$$\frac{\mathrm{d}[\mathbf{IV}]}{\mathrm{d}t} = k_1[\mathbf{IV}]$$

and the backward reaction:

$$\frac{\mathrm{d}[\mathbf{III}]}{\mathrm{d}t} = k_2[\mathbf{III}]\,[\mathrm{Py}]$$

which are related to the NMR exchange-line broadenings Δ_e in the regime of slow exchange as follows [6] [7]:

$$k_1 = \pi\Delta_e$$

$$k_2 = \pi\Delta_e\,[\mathrm{Py}]$$

respecting the constraint: $k_1/k_2 = K$.

K, k_1, k_2, and the corresponding thermodynamic and kinetic parameters $\Delta H°$, $\Delta S°$, $\Delta H_1^{\neq}$, $\Delta S_1^{\neq}$, $\Delta H_2^{\neq}$, and $\Delta S_2^{\neq}$ have been estimated from the series of temperature-dependent ^{1}H-NMR spectra *(Fig. 4)* by a least-squares fit to the observed signal intensities and line widths of the *ortho*-protons of complexed and free pyridine, respectively, at the various temperatures[3]).

[3]) The method used to evaluate the NMR data is simple compared to the 'state of the art' in this field ([7] and ref. cited therein). We think, however, to have extracted the *essential* features of our system, and that a more rigorous treatment of the NMR data would not modify much the results (enthalpies ±1–2 kcal mol^{-1} max.; entropies ±5 cal K^{-1} mol^{-1} max.).

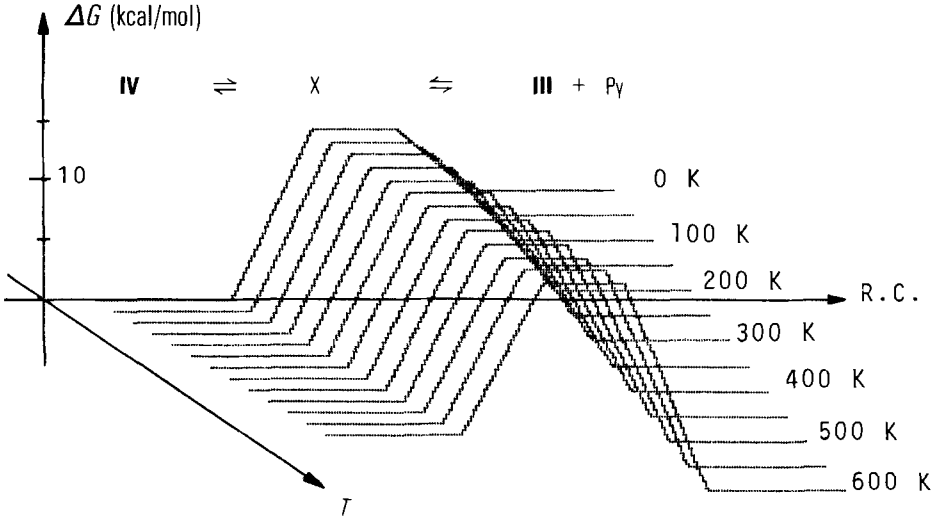

Fig. 7. ΔG Diagram of the reaction **IV**⇌**III** + Py *at standard conditions* (c_0 = 1M): **IV**: $H^\circ = 0$; $S^\circ = 0$ (reference); transition state: $H^\circ = +14.9(10)$ kcal·mol^{-1}, $S^\circ = +2.7(33)$ cal·K^{-1}·mol^{-1}; **III** + Py: $H^\circ = +9.5(10)$ kcal·mol^{-1}, $S^\circ = +24.5(33)$ cal·K^{-1}·mol^{-1}. *ΔG* Diagrams for arbitrary concentrations *c* can be constructed using the formula $\Delta G^* = \Delta H^\circ - T(\Delta S^\circ - R \ln c)$.

The results are summarized in *Fig. 7*. Two conclusions are worth mentioning: *1)* extrapolated to 0 K, **IV** is ~ 10 kcal/mol more stable than **III**, indicating that **III** is considerably strained. At high temperature, the positive entropy (25 · cal · K^{-1} · mol^{-1}) favours dissociation of the adduct; *2)* the entropy of the dissociation reaction is found almost completely on the bimolecular side of the reaction profile, indicating an associative transition state, *i.e.* an S_N2-type mechanism for the nucleophilic substitution.

Discussion of Strain in III. – Some of the strain energy in **III** may be traced to the bond angles within the five-membered chelate rings which are unusually small if compared to those in **IV** *(Table 1)*. It may also be argued that **IV** is stabilized relative to **III** because – as indicated by the C–N distances *(Table 1)* – the N-lone pair in **IV** may partially delocalize onto the Ph rings due to the Ph torsion angles about the C(2)–N bonds of ~ 20° (compared to ~ 3° in **III**). Finally, the B–N distance in **IV** or **III**-quin is 0.04–0.05 Å shorter than in **III**, a fact that may be related to the absence of antiperiplanar lone pairs in **IV** (torsion angle C(1)–O–B–N(1) ~ 140°) as compared to **III** (torsion angle C–O–B–N(1) ~ 5°) and, therefore, to the lack of anomeric lengthening [8] of the B–N(2) bond in **IV**, an effect which is likely to influence the B–N(1) bond in **III**. If it were assumed that the entire difference ΔH° could be explained in terms of the difference Δd of B–N distances in the educt and product, then the ratio $\Delta H^\circ/\Delta d$ would be about 190–240 kcal · mol^{-1} · Å^{-1}. A simple model [9] based on a modified *Morse* potential yields the relationship $\Delta E/\Delta d = -k/a$ where k is the B–N stretching force constant (3–3.5 mdyn Å^{-1} [10]) and a is the *Morse* asymmetry parameter (~ 2 Å^{-1}). The computed value of $\Delta E/\Delta d$ of ~ 210–250 kcal · mol^{-1} · Å^{-1} would compare well with the experimental value and with the ratio $\Delta\Delta G^*/\Delta d$ ~ 250 kcal · mol^{-1} · Å^{-1} for the cleavage of a C–O bond during acetal hydrolysis [11].

Experimental Part

1. *General.* All chemicals were purchased from *Fluka*, unless indicated otherwise. ^{1}H-NMR: chemical shifts in δ[ppm] rel. to TMS. ^{11}B-NMR: chemical shifts in δ[ppm] rel. to $BF_3 \cdot Et_2O$.

2. *2,2',2''-Nitrilotriphenyl Borate* (**III**). A soln. of 1 g of 2,2',2''-nitrilotriphenol (prepared according to [4]) in 10 ml of MeCN was mixed with a soln. of 1 g of $(MeO)_3B$ in 10 ml of MeCN. Immediate precipitation of the product occurred. After 30 min, the white **III** was isolated, washed with MeCN and dried *in vacuo*. M.p. > 200° (sublimation). IR: *Fig. 2a*. ^{1}H-NMR ((D$_8$)THF, 250 MHz): 7.91 (pseudo-*d*, 3 H *o* to N); 7.19 (pseudo-*t*, 3 H *p* to N); 6.91 (pseudo-*d*, 3 H *o* to O); 6.85 (pseudo-*t*, 3 H *p* to O); assignments based on [6] [12]. ^{11}B-NMR ((D$_8$)THF, 80.25 MHz): +19.4 (*s*). Anal. calc. for $C_{18}H_{12}BNO_3$ (301.113): C 71.80, H 4.02, N 4.65; found: C 71.40, H 3.95, N 4.88.

Single crystals of **III**, suitable for X-ray-structure analysis, were obtained from the reaction mixture when the synthesis was carried out in DMSO at 80°.

3. *2,2',2''-Nitrilotriphenyl (^{10}B) Borate* (^{10}B-**III**). A mixture of 0.61 g of (^{10}B)boric acid (commercially available, 95% enriched $^{10}B(OH)_3$) and 3 g of 2,2',2''-nitrilotriphenol [4] was refluxed with 50 ml of toluene in a 100-ml flask adapted for azeotropic distillation. After the production of H_2O had stopped, toluene was distilled off, and the residue was sublimed at 0.05 Torr (sublimation tube heated to 300°), giving a small zone of unreacted nitrilotriphenol at lower condensation temp., followed by a zone of white crystals of ^{10}B-**III** (2.9 g, 90%). IR: 3060*w*, 3030*vw*, 1610*m*, 1605*w* (sh), 1590*w* (sh), 1490*vs*, 1470*vs*, 1325*vs*, 1320*m* (sh), 1300*m*, 1280*m*, 1270*m*, 1250*s*, 1205*vs*, 1195*vs*, 1160*w*, 1120*vs*, 1115*s* (sh), 1090*vs*, 1070*vs*, 1045*m*, 1025*m*, 975*w*, 930*m*, 920*m*, 880*s*, 830*w*, 790*w*, 755*vs*, 745*s*, 700*w*, 620*m*, 460*m*, 385*w*, 355*w*, 325*w*. Anal. calc. for $C_{18}H_{12}{}^{10}BNO_3$ (300.352): C 71.98, H 4.03, N 4.66; found: C 72.73, H 4.05, N 4.70.

4. *Quinuclidine-2,2',2''-nitrilotriphenoxyborane* (**III**-quin). A soln. of 1 g of 2,2',2''-nitrilotriphenol [4] in 10 ml of MeCN was mixed with a soln. of 1.1 g of quinuclidine and 1 g of $(MeO)_3B$ in 10 ml of MeCN. Overnight, colourless, well developed crystals separated which were washed with MeCN and dried *in vacuo*. 1.34 g (95%). The compound is only sparingly soluble in common aprotic solvents. M.p. (dec.) *ca.* 200°. IR: 3060*w*, 3025*w*, 3005*w*, 2980*w*, 2960*w*, 2950*w*, 2940*w*, 2900*w*, 2880*w*, 1605*m*, 1590*w*, 1570*w*, 1485*s*, 1460*m*, 1425*w*, 1380*w*, 1355*w*, 1345*w*, 1305*s*, 1280*s* (sh), 1275*s*, 1255*m*, 1225*w*, 1210*w*, 1170*w*, 1145*w*, 1125*w*, 1105*w*, 1095*m*, 1080*m*, 1065*s* (sh), 1050*s*, 1040*s*, 1025*s*, 950*m*, 940*s*, 915*w*, 910*w*, 860*m*, 845*m*, 830*m*, 820*m*, 815*m*, 800*w*, 790*w*, 760*s*, 745*m*, 715*w*, 685*w*, 650*w*, 625*m*, 610*w*, 540*w*, 520*m*, 490*w*, 470*m*, 380*w*, 360*w*. Anal. calc. for $C_{25}H_{25}BN_2O_3$ (412.302): C 72.83, H 6.11, N 6.79; found: C 72.76, H 6.21, N 6.94.

5. *Diazabicyclooctane-2,2',2''-nitrilotriphenoxyborane* (**III**-DABCO) was prepared by substituting DABCO for quinuclidine in the above prescription: fine, white powder, very sparingly soluble in common aprotic solvents. M.p. (dec.) *ca.* 200°. IR: 3100*vw*, 3070*w*, 3040*w*, 3020*w*, 2960*vw*, 2940*vw*, 1645*vs*, 1610*m*, 1595*w*, 1580*m* (sh), 1565*s*, 1535*m*, 1490*vs*, 1460*s*, 1440*m*, 1420*vw*, 1400*m*, 1340*w*, 1305*vs*, 1290*m* (sh), 1280*s*, 1260*m*, 1230*s*, 1210*w*, 1160*w*, 1150*vw*, 1135*m*, 1110*vs*, 1100*vs* (sh), 1070*m*, 1050*vs*, 1030*s*, 1005*vs*, 990*s*, 955*s*, 940*vs*, 920*m* (sh), 865*m*, 835*m*, 810*s*, 760*vs*, 745*m* (sh), 715*m*, 670*w*, 625*m*, 565*w*, 535*m*, 515*w*, 500*w*, 470*w*. Anal. calc. for $C_{24}H_{24}BN_3O_3$ (413.29): C 69.75, H 5.85, N 10.17; found: C 69.33, H 5.96, N 10.50.

6. *4-(Dimethylamino)pyridine-2,2',2''-nitrilotriphenoxyborane* (**III**-Me_2NPy). A soln. of 1 g of 2,2',2''-nitrilotriphenol [4] in 10 ml of MeCN was mixed with a soln. containing 1 g of 4-(dimethylamino)pyridine and 1 g of $(MeO)_3B$. On mixing, a voluminous, white precipitate was formed which dissolved again within a few min. Then, plate-like crystals separated which were washed with MeCN and dried *in vacuo*. Yield 80%. IR: 3060*w*, 3020*w*, 3010*vw*, 2990*vw*, 2980*w*, 2950*w*, 2940*w*, 2900*vw*, 2880*w*, 1600*m*, 1590*w*, 1570*w*, 1490*vs*, 1460*s*, 1375*w*, 1330*w* (sh), 1305*vs*, 1280*s* (sh), 1270*s*, 1255*m*, 1225*vw*, 1180*vw*, 1150*w*, 1110*m*, 1095*m*, 1085*m*, 1070*s* (sh), 1055*vs*, 1045*vs*, 1030*s*, 1015*w* (sh), 1010*w* (sh), 990*m*, 945*s* (sh), 935*vs*, 915*w* (sh), 905*vw* (sh), 865*m* (sh), 860*s*, 835*m*, 820*m*, 800*w*, 765*vs*, 750*m*, 715*w*, 680*w*, 630*m*, 520*w*, 470*w*, 380*w*, 360*w*. Anal. calc. for $C_{25}H_{22}BO_3N_3$ (423.285): C 70.94, H 5.24, N 9.93; found: C 64.21, H 4.71, N 8.70. The absolute values found are too small, but the ratio of the 3 elements is correct; we suspect contamination of the sample for analysis by an inert solid such as glass.

7. *Pyridine-2,2',2''-nitrilotriphenoxyborane* (**III**-Py = **IV**). By substituting pyridine for 4-(dimethylamino)pyridine in the above prescription, plate-like crystals of **III**-Py were obtained: 1.17 g (90.5%). On heating, the crystals decomposed by loosing pyridine. IR: *Fig. 2b*. ^{1}H-NMR ((D$_8$)THF, 250 MHz, 210 K; *Fig. 3a*): signals due to complexed pyridine: 9.27 (pseudo-*d*, 2 H$_o$); 7.98 (pseudo-*t*, 2 H$_m$); 8.44 (pseudo-*t*, H$_p$); *cf.* signals of free pyridine in (D$_8$)THF at 8.59, 7.38, and 7.75, resp.; signals due to nitrilotriphenoxyborane: 7.32 (pseudo-*d*, 3 H *o* to N); 6.96 (pseudo-*t*, 3 H *p* to N); 6.82 (pseudo-*d*, 3 H *o* to O); 6.76 (pseudo-*t*, 3 H *p* to O). ^{1}H-NMR ((D$_8$)THF, 250

MHz, 350 K; *Fig. 3b*): signals due to pyridine: 8.55 (pseudo-*d*, 2 H_o); 7.24 (pseudo-*t*, 2 H_m); 7.65 (pseudo-*t*, H_p); signals due to nitrilotriphenoxyborane: 7.87 (pseudo-*d*, 3 H *o* to N); 7.18 (pseudo-*t*, 3 H *p* to N); 6.89 (pseudo-*d*, 3 H *o* to O); 6.84 (pseudo-*t*, 3 H *p* to O). ^{11}B-NMR ((D$_8$)THF, 80.25 MHz): *s* at +5.6 (210 K) and +18.8 (350 K). Anal. calc. for $C_{23}H_{17}BN_2O_3$ (380.216): C 72.66, H 4.51, N 7.37; found: C 72.56, H 4.48, N 7.53.

Crystals for X-ray-structure determination were obtained by slow cooling of a sat. soln. of the complex in pyridine (200 mg of **III**-Py = **IV** in 2 ml of pyridine) from 90° to r.t. at a rate of 10°/day.

8. *Pyridine-2,2',2''-nitrilotriphenoxy(*^{10}*B)borane* (^{10}**B-III**-Py) was obtained in a similar manner: 1 g of ^{10}**B-III** was dissolved in *ca.* 6 ml of refluxing pyridine. On cooling, plate-like crystals of ^{10}**B-III**-Py separated which were isolated and dried *in vacuo*: 1.1 g. IR: 3080*w*, 3040*w*, 1630*m*, 1610*m*, 1590*m*, 1580*m*, 1505*m* (sh), 1500*s* (sh), 1490*vs*, 1460*s*, 1455*m* (sh), 1445*m* (sh), 1360*w*, 1305*vs*, 1285*m* (sh), 1280*s*, 1255*w*, 1245*w*, 1220*vw*, 1215*w* (sh), 1210*m*, 1160*w*, 1120*s*, 1110*m* (sh), 1100*vs*, 1090*m*, 1065*m*, 1050*vs*, 1035*s*, 1025*m*, 1005*w*, 945*vs*, 870*w*, 860*w*, 830*m*, 815*w* (sh), 795*w*, 775*s* (sh), 765*s*, 750*m*, 745*m* (sh), 735*w* (sh), 720*w*, 705*m*, 690*s*, 630*m*, 530*w*, 480*w*, 355*w*. Anal. calc. for $C_{23}H_{17}{}^{10}BN_2O_3$ (379.504): C 72.81, H 4.52, N 7.38; found: C 72.24, H 4.54, N 7.39 (average of two determinations).

9. *Temperature-Dependent X-Ray Powder Diagrams* were taken on a *'Nonius'-Guinier-Lenné* camera [13] using CuK_α radiation (curved quartz monochromator plate). The camera allowed for diffraction angles $0 < \theta \leqslant 42°$. The vertical beam length was 5 mm. Finely powdered samples were pressed onto Pt sieves (area 2 cm^2) which were inserted into the camera. Temp. was controlled with N_2 gas. It was increased from r.t. to *ca.* 250° at a rate of 25°/h, coupled with a vertical movement of the film plate of 10 mm/h. On the exposures, 4 Pt diffraction lines are present, at θ = 19.89, 23.14, 33.76, 40.66°, which can serve for calibration purposes. The first 3 of them are marked by little arrows in *Fig. 1*.

10. *Temperature-Dependent* ^{1}*H-NMR Spectra.* Sample preparation was complicated by the low solubility of **IV** and its tendency to hydrolyze even with traces of H_2O present in the solvent. (D$_8$)THF (*Merck*, 98.5% deuterated, dried over $LiAlH_4$) was finally chosen as solvent. The sample preparation was carried out using *Schlenk* techniques. NMR tubes of 5 mm diameter fitted with glass joints and stoppers were used. A single crystal of **IV** was weighed in a dried NMR tube of known weight, and the tube attached to the vacuum line. A 10-ml flask, containing 2 ml of (D$_8$)THF with a little $LiAlH_4$ was also connected to the vacuum line. After 2 h of magnetic stirring at r.t., the (D$_8$)THF was distilled under vacuum to a second flask cooled with liq. N_2. From there, part of the (D$_8$)THF was distilled into the NMR tube by the same technique. The NMR tube was then filled with N_2 (gas), detached from the line, immediately fitted with its stopper and weighed. Then the tube was sealed off and the glass joint removed. The weight of **IV** was 2.985 mg and that of (D$_8$)THF 597.1 mg (density of (D$_8$)THF at 20°, 0.9878 g/cm^3). The concentration of **IV** was calculated to be 0.0130 mol/l. From this sample, the whole series of 250-MHz ^{1}H-NMR spectra[4]) (*Fig. 3* and *4*) as well as the series of 80.25-MHz ^{11}B-NMR spectra were obtained.

11. *Estimation of Thermodynamic and Kinetic Parameters*[3]). The *m* of the 2 H_o of pyridine does not overlap with other signals, neither in complexed nor in free pyridine. The frequency difference between the two exchange related signals is high enough ($\sim$ 175 Hz) to result in slow exchange spectra over a large part of the studied temp. range (210–300 K). The widths of the individual NMR resonances Δ_1(**IV**) and Δ_2(Py) were estimated from the measured overall widths of the *m* using a series of simulated spectra based on convolution of the known pyridine line spectrum [12] and an increasing line-width function. The integral ratio *x* was calculated from the integrals of the corresponding signals of complexed and free pyridine (*Table 2*).

The observed mol fraction *x* and line widths Δ_1 and Δ_2 are related to the thermodynamic and kinetic parameters through the following equations:

$$x = [(c_0 p - K) + \sqrt{(c_0 p - K)^2 + 4\, c_0 K}]/2\, c_0$$

where:

$$K = \exp[(\Delta H_2^{\neq} - \Delta H_1^{\neq})/RT - (\Delta S_2^{\neq} - \Delta S_1^{\neq})/R]$$

$$\Delta_1 = \Delta_a + (k_b \cdot T/\pi \cdot h) \cdot \exp(\Delta H_1^{\neq}/RT + \Delta S_1^{\neq}/R)$$

$$\Delta_2 = \Delta_b + (k_b \cdot T/\pi \cdot h) \cdot (x - p) \cdot c_0 \cdot \exp(-\Delta H_2^{\neq}/RT + \Delta S_2^{\neq}/R)$$

(k_b = *Boltzmann*'s constant; h = *Planck*'s constant)

x is the experimental integral ratio and c_0 the initial concentration of **IV**. Δ_1 and Δ_2 are the observed line widths of the signals of the 2 H_o of complexed and free pyridine, respectively. In addition to the 4 independent reaction parameters $\Delta H_1^{\neq}$, $\Delta H_2^{\neq}$, $\Delta S_1^{\neq}$, and $\Delta S_2^{\neq}$, 3 additional quantities are necessary: Δ_a and Δ_b account for contribu-

[4]) The digitalized ^{1}H-NMR spectra from 210 K to 350 K are available on punched paper tape.

Table 2. *Experimental and Calculated NMR-Line Width of the 2 H_0 of Pyridine in* **IV** *and Free Pyridine, mol Fraction of* **III** *as a Function of* T

T [K]	**IV**				**III** + pyridine				mol Fractions[b])		
	m width [Hz]	$\Delta_1^{obs.a)}$	$\Delta_1^{calc.}$	w	m width [Hz]	$\Delta_2^{obs.a)}$	$\Delta_2^{calc.}$	w	$x^{obs.}$	$x^{calc.}$	w
210	9.37	1.75	1.74	1	8.75	1.00	1.00	1	0.093	0.086	50
220	9.62	2.00	1.75	1	8.88	1.25	1.05	1	0.114	0.112	50
230	9.88	2.25	1.78	1	9.37	1.50	1.20	1	0.142	0.152	50
240	9.88	2.25	1.89	1	9.34	1.50	1.58	1	0.197	0.207	50
250	10.06	3.50	2.30	2	10.31	3.00	2.44	2	0.283	0.279	100
260	11.38	5.00	3.60	2	11.25	4.75	4.22	2	0.369	0.366	100
270	15.31	11.00	7.38	2	13.38	8.00	7.52	2	0.446	0.463	100
280	22.40	19.50	17.56	2	19.69	16.50	13.17	2	0.560	0.565	100
290	44.06	41.50	43.13	2	26.12	23.75	22.06	2	0.691	0.663	100
300	..	–	–	–	40.94	37.50	35.08	2	0.826	0.749	100

a) $\Delta_1^{obs.}$, $\Delta_2^{obs.}$ obtained from m widths with the help of an empirical correlation diagram (see text).
b) See text.

tions to the line widths which are not due to chemical exchange, and p accounts for residual hydrolysis which would irreversibly eliminate some **IV** and produce an amount $c_0 \cdot p$ of excess pyridine: **IV** + $H_2O \rightarrow$ **V** + Py. The 7 adjustable parameters in the 3 non-linear observational equations were determined by a linearized, weighted *Marqardt* least-squares algorithm[5]): $\Delta H_1^{\neq} = 14.9(1.0)$ kcal·mol^{-1}, $\Delta H_2^{\neq} = 5.4(8)$ kcal·mol^{-1}, $\Delta S_1^{\neq} = 2.7(3.3)$ cal·mol^{-1} K^{-1}, $\Delta S_2^{\neq} = -21.8(2.7)$ cal·mol^{-1}·K^{-1}, $\Delta_a = 1.7(8)$ Hz, $\Delta_b = 1.0(8)$ Hz, $p = 0.06(3)$. Correlation coefficients were 0.9997 between $\Delta H_1^{\neq}$ and $\Delta S_1^{\neq}$, 0.9990 between $\Delta H_2^{\neq}$ and $\Delta S_2^{\neq}$, and *ca.* 0.78 between $\Delta H_1^{\neq}$, $\Delta S_1^{\neq}$ on the one hand and $\Delta S_2^{\neq}$, $\Delta S_2^{\neq}$ on the other. All other correlation coefficients were < 0.6. The final agreement factor was $R_w = [(\sum_i w_i \Delta_i^2)/(\sum_i w_i x_i^2 + \sum_i w_i \Delta_1^2 + \sum_i w_i \Delta_2^2)]^{1/2} = 0.074$ (29 observations, 7 variables; e.s.d.'s in parentheses, in terms of the least significant digit). The absolute errors may be about a factor of two larger than indicated by the estimated standard deviations[3]), also because of the large, inherent correlation in extrapolating the ΔS and ΔH values at $1/T = 0$. This problem has been discussed by *Binsch* and *Kessler* [13]. The magnitude of the reaction entropy $\Delta S°$ (25 cal·mol^{-1}·K^{-1}) compares well with those of similar reactions [14].

We thank Prof. *J. D. Dunitz* for permission to use his X-ray diffractometer, Dr. *P. S. Pregosin* for allocation of measurement time on the 250-MHz NMR spectrometer, as well as Dr. *P. Boron* for her practical help in the recording of the NMR spectra. We are also indebted to Dr. *G. Kahr* (Tonmineralogisches Labor, ETHZ) for the recording of temperature-dependent X-ray powder diagrams. *E. M.* thanks the *Schweizerischer Nationalfonds zur Förderung der wissenschaftlichen Forschung* for financial support. Finally, we thank Dr. *R. Kunz* for the computer simulation of various NMR spectra.

5) An adapted version of the least-squares program of *T. Baumeister* und *D. W. Marqardt*, IBM Share Distribution No. 1428 was used.

REFERENCES

[1] R. Mattes, D. Fenske, K. F. Tebbe, *Chem. Ber.* **1972,** *105,* 2089.
[2] E. Müller, H.-B. Bürgi, *Helv. Chim. Acta* **1984,** *67,* 399.
[3] S. Geller, *J. Chem. Phys.* **1960,** *32,* 1569.
[4] C. L. Frye, G. A. Vincent, G. L. Hauschildt, *J. Am. Chem. Soc.* **1966,** *88,* 2727.
[5] E. Müller, H.-B. Bürgi, *Helv. Chim. Acta* **1987,** *70,* 511.
[6] H. Günther, 'NMR-Spektroskopie', Georg Thieme Verlag, Stuttgart, Chapt. VIII. 1973.
[7] M. Feigel, H. Kessler, *Chem. Ber.* **1979,** *112,* 3715.
[8] A. J. Kirby, 'The Anomeric Effect and Related Stereoelectronic Effects at Oxygen', Springer, Berlin, 1983.
[9] H.-B. Bürgi, J. D. Dunitz, *J. Am. Chem. Soc.*, in press.
[10] P. H. Laswick, R. C. Taylor, *J. Mol. Struct.* **1976,** *34,* 197.
[11] A. J. Kirby, P. G. Jones, *J. Am. Chem. Soc.* **1981,** *106,* 6207.
[12] T. Clerc, E. Pretsch, 'Kernresonanzspektroskopie, Teil 1: Protonenresonanz', Akad. Verlagsgesellschaft, Frankfurt am Main, 1973.
[13] G. Binsch, H. Kessler, *Angew. Chem.* **1980,** *92,* 445.
[14] J. J. Christensen, D. J. Eatough, R. M. Izatt, 'Handbook of Metal Ligand Heats', 2nd edn., Marcel Dekker Inc., New York.